Modeling of Nonlinear Polyurethane Production in Batch Reactors Using a Kinetic−Probabilistic Approach

Eduardo Vivaldo-Lima,*,† Gabriel Luna-Bárcenas,‡ Antonio Flores-Tlacuahuac,§ M. Amelia Cruz,|| and Octavio Manero⊥

Departamento de Ingeniería Química, Facultad de Química, Universidad Nacional Autónoma de México (UNAM), Conjunto E, Ciudad Universitaria, México D. F., CP 04510, México, Centro de Investigación y Estudios Avanzados (CINVESTAV), IPN, Unidad Querétaro, Querétaro, México, Departamento de Ingeniería y Ciencias Químicas, Universidad Iberoamericana (UIA), Lomas de Santa Fé, México D. F., CP 01210 México, CID Centro de Investigación y Desarrollo Tecnológico S. A. de C. V., Avenida de los Sauces 87, Manzana 6, Parque Industrial Lerma, Estado de México, CP 52000 México, and Instituto de Investigaciones en Materiales (IIM), Universidad Nacional Autónoma de México (UNAM), Ciudad Universitaria, México D. F., CP 04510 México

The nonlinear step-growth copolymerization of a mixture of low- and high-molecular-weight diols, and a low-molecular-weight diisocyanate is addressed using a kinetic−probabilistic model. The kinetic model allows for the calculation of the concentrations of all species. Different reactivities for isocyanate functional groups located in different positions of the monomer and polymer molecules, as well as the hydroxyl functional groups of different molecules, are allowed. A recursive probabilistic model is used to calculate the number- and weight-average molecular masses. Allophanate and biuret ramification reactions, as well as gelation formation due to cross-linking, are considered in the model. The model is validated for the reaction of methyl diisocyanate (MDI) with a mixture of a polyester and 1,4-butanediol. Agreement between the model predictions and experimental data from the literature on diol conversion, weight-average molecular weight, and reaction mixture viscosity is satisfactory.

Introduction

Polyurethanes have been in the market for over 60 years. Their uses and applications are quite diverse. Created initially to rival polyamide (nylon) fibers, they are now important in fields such as flexible and rigid foams, elastomers, coatings, and adhesives, as well as in medical applications. Heart pacers, implants, artificial hearts, casts, etc., are usually made out of polyurethane-based materials.[1,2]

The design, modeling, optimization and control of polymerization processes are active research areas and are part of a well-established discipline known as polymer reaction engineering. The development of effective mathematical models with predictive power is a major issue in this area. Several mathematical techniques are available for kinetics and molecular weight development modeling in step-growth and chain-growth polymerizations.[3−5] They usually work well for linear polymers, but their direct application to the production of nonlinear polymers is at most an approximation to the actual behavior of these systems. The predictive power of these models decreases when cross-linking reactions are considered.

The main statistical theories used to model gelation in step-growth polymerization are the Flory−Stockmayer classical theory,[6−9] the Macosko−Miller conditional probability model,[10−13] and Gordon's cascade theory.[14] As applied to the modeling of network formation in production of polyurethanes in recent years, Sekkar et al.[15] used a model based on the classical theory; the group of Dušek[16−18] used and improved the theory of Gordon, and Gupta and Kumar adapted the Macosko−Miller model to nonlinear polyurethane production with different reactivities of isocyanate functional groups.[3] The Macosko−Miller model has also been used for polyurethane production modeling assuming equal reactivities of the functional groups.[19−21] More recently, Miller and Sarmoria[22,23] reviewed and enhanced the Macosko−Miller recursive probabilistic modeling approach. Most publications with a quantitative view of the production of polyurethanes and other step-growth resins have used simplified kinetic expressions to calculate the concentrations of all species involved in the polymerization. The reaction rate is usually given by the product of a single kinetic constant with the concentration of one reactant (e.g., isocyanate functional group) raised to a reaction order and the concentration of the other reactant (e.g., hydroxyl functional group) raised to its respective reaction order,[24−28] with the assumption of equal reactivities for each functional group, regardless of position or size on the monomer or polymer molecules.

The interest of our group in the modeling of nonlinear polyurethane production has centered on implementing an effective model for molecular weight development. An adequate prediction of the gelation point is sought. Effectiveness is understood as a compromise between predictive power and ease of solution of the governing equations. The goal is to develop an effective mathematical model for industrial application.

* To whom correspondence should be addressed. E-mail: vivaldo@servidor.unam.mx. Fax: +5255-5622-5355.

† Departamento de Ingeniería Química, Universidad Nacional Autónoma de México (UNAM).

‡ Centro de Investigación y Estudios Avanzados (CINVESTAV), Unidad Querétaro.

§ Universidad Iberoamericana (UIA).

|| CID Centro de Investigación y Desarrollo Tecnológico S. A. de C. V.

⊥ Instituto de Investigaciones en Materiales (IIM), Universidad Nacional Autónoma de México (UNAM).

10.1021/ie010742g CCC: $22.00
Published on Web 09/12/2002

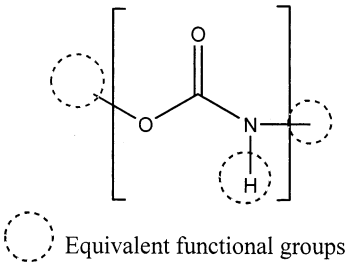

Figure 1. Urethane functional group. Dotted circles show equivalent functionalities, if considered as a monomer unit.

After detailed analysis of the theories and models available in the literature, two approaches were considered: (a) adaptation of the Macosko−Miller recursive probabilistic model for molecular weight averages to our reaction system and (b) development of mathematical expressions for moments of the molecular weight distribution using the method of moments. Both approaches are adequate for the development of models with predictive power and reasonable degrees of complexity. The results of strategy a and comparison with experimental data from the literature are reported in this paper. Development and reporting of strategy b will be the scope of another publication.

Although the model developed and implemented here allows for the presence of a diamine and a multiol cross-linker (a molecule with more than two hydroxyl functional groups), the calculations in the Results and Discussion section consider only the reaction of a diisocyanate, a diol of low molecular weight, and a diol of high molecular weight. The emphasis is on cross-linking and the possibility of gelation due to allophanate formation.

Branching and Cross-Linking in Polyurethane Production of $A_2 + B_2$ Monomers

It is well-known that the step-growth polymerization of $A_2 + B_2$ monomers, where the subscript 2 refers to monomer functionality, leads to linear molecules. The functionality of at least one of the monomers has to be 3 or higher to produce nonlinear molecules. However, in polyurethane production, where the monomers are diisocyanate and diol molecules, the production of nonlinear polymer, and even a polymer network, is possible. This is due to the formation of an allophanate functional group when an isocyanate group reacts with a urethane functional group. If an amime functional group is present in the system, the reaction between isocyanate and amine produces a urea functional group. The reaction between the urea and the isocyanate functional groups produces the biuret functional group.

Figures 1 and 2 show the chemical structures of the urethane and urea repeat units of a polyurethane molecule. The dotted circles in the figures show the equivalent functionalities of these units. Branching, cross-linking, and gelation are modeled in this paper assuming that the urethane repeating unit behaves as a monomer of functionality 3 (the third functional group being the proton attached to the nitrogen atom). Likewise, the urea repeat unit is modeled as a monomer of functionality 4, as observed in Figure 2 (two protons attached to the two nitrogen atoms of the urea group).

Figure 3 shows the reaction mechanism that produces urethane and allophanate functional groups. One of the isocyanate groups of the diisocyanate monomer reacts

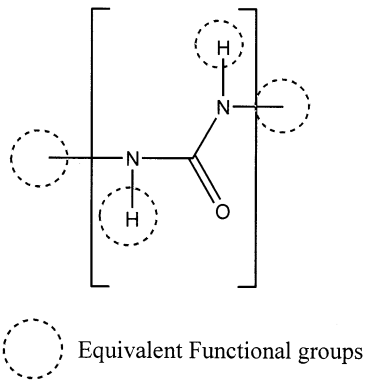

Figure 2. Urea functional group. Dotted circles show equivalent functionalities, if considered as a monomer unit.

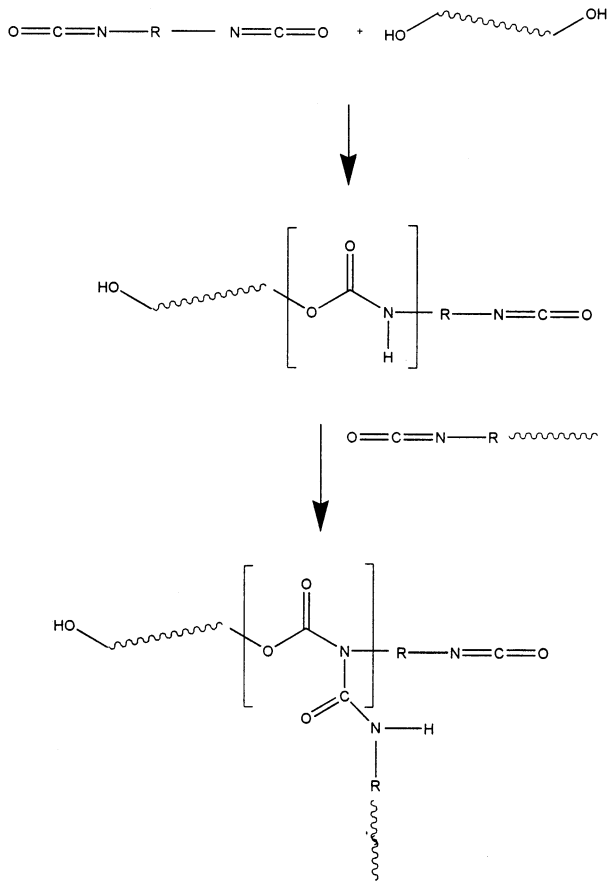

Figure 3. Schematic representation of the reaction mechanism for the production of urethane and allophanate units in polyurethane production.

with one of the hydroxyl groups of the diol to produce a urethane functional group and a molecule with isocyanate and hydroxyl chain ends. In the system modeled later, two types of diols are considered, a high-molecular-weight diol (a polyester molecule) and a low-molecular-weight diol (1,4-butanediol). The diol molecule represented in the upper reaction of Figure 3 is the high-molecular-weight diol, but it could be the low-molecular-weight one.

The proton attached to the nitrogen atom of the urethane functional group can be attacked by an isocyanate functional group to produce an allophanate group, as shown in the second reaction of Figure 3. As observed, the formation of the allophanate functional group generates a branch on the main polymer chain.

These reactions can proceed, producing more branching and cross-linking. Eventually, a polymer network can be obtained. The reactions between isocyanate and amine functional groups to produce the urea functional group and the further reaction between the urea and isocyanate functional groups to produce a biuret (another branching reaction) are not shown, but they are similar to the reactions with the hydroxyl functional group. The reactions with a diamine will not be analyzed in this paper, but they are included in the mathematical model and the computer program that solves the model equations.

Modeling

The model used in this paper consists of a set of kinetic equations that describe the rates of consumption or formation of all of the species present in the system and a set of algebraic equations, an application of the recursive probabilistic model of Macosko and Miller[10−13] to this reacting system, which allows for the calculation of the molecular weight averages and the gelation point.

Kinetic Description of the System. The reaction scheme used here is similar to that used by Gupta and Kumar,[3] except for the reactions with a low-molecular-weight diol (B′−B′), which they did not consider. Another difference is that, in our reaction scheme, hydroxyl groups from different reagents are allowed to have different reactivities. However, all hydroxyl groups of a single molecule have the same reactivity. The reaction scheme, eqs 1−24, is shown below. Note that, in these equations, a horizontal line represents a polymer chain, and a superscript * on a functional group indicates that the functional group is bound to a polymer chain. Thus, −A* represents a polymer chain with an A end group, and −AB− represents the linkage of an A functional group with a B functional group located at an intermediate position within a polymer chain.

$$A_2A_1 + B- \xrightarrow{k_1} {}^*A_2A_1B- \text{ (E)} \quad (1)$$

$$A_1A_2 + B- \xrightarrow{k_2} {}^*A_1A_2B- \text{ (E)} \quad (2)$$

$$-A_1{}^* + B- \xrightarrow{k_1^*} -A_1B'- \text{ (E)} \quad (3)$$

$$-A_2{}^* + B- \xrightarrow{k_2^*} -A_2B'- \text{ (E)} \quad (4)$$

Equations 1−4 show the four different reactions between isocyanate (A) and hydroxyl (B) functional groups from a diol of high molecular weight to produce a urethane functional group (E). Depending on the values of the kinetic rate constants k_1, k_2, k_1^*, and k_2^*, the cases of equal or unequal reactivities of the isocyanate functional group can be modeled. It is assumed that functional groups bound to a polymer molecule (as indicated by a superscript *) are less reactive than those from a monomer molecule.

Equations 5−8 show the equivalent reactions, but in this case the diol is a low-molecular-weight molecule (B′).

$$A_2A_1 + B'- \xrightarrow{k_3} {}^*A_2A_1B'- \text{ (E)} \quad (5)$$

$$A_1A_2 + B'- \xrightarrow{k_4} {}^*A_1A_2B'- \text{ (E)} \quad (6)$$

$$-A_1{}^* + B'- \xrightarrow{k_3^*} -A_1B'- \text{ (E)} \quad (7)$$

$$-A_2{}^* + B'- \xrightarrow{k_4^*} -A_2B'- \text{ (E)} \quad (8)$$

Equations 9−12 show the reactions between isocyanate and hydroxyl functional groups. However, in this case the hydroxyl functional group comes from an *f*-functional multiol. The reactivities of the hydroxyl functional groups can differ depending on whether they belong to a polyester, to a diol of low molecular weight, or to a multiol molecule.

Equations 13−16 show the reactions of the different isocyanate functional groups with an amine functional group from a diamine monomer to produce a polyurea (F). The formation of allophanate functional groups (M) is represented by eqs 17−20. Equations 21−24 show the reactions leading to the formation of biuret functional groups from isocyanate and urea functional groups.

$$A_2A_1 + B_{f-1}- \xrightarrow{k_9} {}^*A_2A_1B_{f-2}- \text{ (E)} \quad (9)$$

$$A_1A_2 + B_{f-1}- \xrightarrow{k_{10}} {}^*A_1A_2B_{f-2}- \text{ (E)} \quad (10)$$

$$-A_1{}^*B_{f-1}- \xrightarrow{k_9^*} -A_2B_{f-2}- \text{ (E)} \quad (11)$$

$$-A_2{}^*B_{f-1}- \xrightarrow{k_{10}^*} -A_2B_{f-2}- \text{ (E)} \quad (12)$$

$$A_2A_1 + D \xrightarrow{k_5} {}^*A_2A_1D- \text{ (F)} \quad (13)$$

$$A_1A_2 + D \xrightarrow{k_6} {}^*A_1A_2D- \text{ (F)} \quad (14)$$

$$-A_1{}^* + D \xrightarrow{k_5^*} -A_1D- \text{ (F)} \quad (15)$$

$$-A_2{}^* + D \xrightarrow{k_6^*} A_2D- \text{ (F)} \quad (16)$$

$$A_2A_1 + E \xrightarrow{R_3k_1} M\ (+\ {}^*A_2-) \quad (17)$$

$$A_1A_2 + E \xrightarrow{R_3k_2} M\ (+{}^*A_1-) \quad (18)$$

$$-A_1{}^* + E \xrightarrow{R_3k_1^*} M \quad (19)$$

$$-A_2{}^* + E \xrightarrow{R_3k_2^*} M \quad (20)$$

$$A_2A_1 + F \xrightarrow{k_7} G\ (+\ {}^*A_2-) \quad (21)$$

$$A_1A_2 + F \xrightarrow{k_8} G\ ({}^*A_1-) \quad (22)$$

$$-A_1{}^* + F \xrightarrow{k_7^*} G \quad (23)$$

$$-A_2{}^* + F \xrightarrow{k_8^*} G \quad (24)$$

In the reaction scheme above, A_1A_2 represents a diisocyanate monomer molecule. The subscripts 1 and 2 identify each of the isocyanate groups belonging to the diisocyanate molecule. As stated before, a superscript * on a functional group indicates that the functional group is bound to a polymer chain. When attached to a kinetic constant, the superscript indicates the reactivity of the functional group attached to a polymer chain, as opposed to that of a functional group belonging

to a monomer molecule. B represents a hydroxyl functional group from the polyester. B′ is a hydroxyl functional group from 1,4-butanediol (low-molecular-weight extender). A diol molecule is made of two hydroxyl functional groups (B−B), and a diisocyanate molecule consists of two isocyanate functional groups. D is amine functional group from a diamine (D−D) molecule. E, M, F, and G represent the urethane, allophanate, urea, and biuret functional groups, respectively.

R_3 is a constant that indicates that the rate of allophanate formation is proportional to the rate of urethane production. In other words, the reactivity of an isocyanate functional group with a proton from the urethane group is proportional to the reactivity of an isocyanate group with a hydroxyl functional group.

From the reaction scheme represented by eqs 1−24, the following kinetic equations can be derived

$$\frac{d[A_1]}{dt} = -k_1[A_1]([B] + R_3[E]) - k_3[A_1][B'] - k_9[A_1][B_f] - k_5[A_1][D] - k_7[A_1][F] \quad (25)$$

$$\frac{d[A_2]}{dt} = -k_2[A_2]([B] + R_3[E]) - k_4[A_2][B'] - k_{10}[A_2][B_f] - k_6[A_2][D] - k_8[A_2][F] \quad (26)$$

$$\frac{d[A_1^*]}{dt} = k_2[A_2][B] + k_4[A_2][B'] + k_6[A_2][D] + R_3k_2[A_2][E] + k_8[A_2][F] + k_{10}[A_2][B_f] - k_1^*[A_1^*][B] - R_3k_1^*[A_1^*][E] - k_3^*[A_1^*][B'] - k_5^*[A_1^*][D] - k_7^*[A_1^*][F] - k_9[A_1^*][B_f] \quad (27)$$

$$\frac{d[A_2^*]}{dt} = k_1[A_1][B] + k_3[A_1][B'] + k_5[A_1][D] + R_3k_1[A_1][E] + k_7[A_1][F] + k_9[A_1][B_f] - k_2^*[A_2^*][B] - R_3k_2^*[A_2^*][E] - k_4^*[A_2^*][B'] - k_6^*[A_2^*][D] - k_8^*[A_2^*][F] - k_{10}[A_2^*][B_f] \quad (28)$$

$$\frac{d[B]}{dt} = -(k_1[A_1] + k_2[A_2])[B] - k_1^*[A_1^*][B] - k_2^*[A_2^*][B] \quad (29)$$

$$\frac{d[B']}{dt} = -(k_3[A_1] + k_4[A_2])[B'] - k_3^*[A_1^*][B'] - k_4^*[A_2^*][B'] \quad (30)$$

$$\frac{d[B_f]}{dt} = -(k_9[A_1] + k_{10}[A_2])[B_f] - k_9^*[A_1^*][B_f] - k_{10}^*[A_2^*][B_f] \quad (31)$$

$$\frac{d[D]}{dt} = -(k_5[A_1] + k_6[A_2])[D] - k_5^*[A_1^*][D] - k_6^*[A_2^*][D] \quad (32)$$

$$\frac{d[E]}{dt} = (k_1[A_1] + k_2[A_2])[B] + k_1^*[A_1^*][B] + k_2^*[A_2^*][B] + (k_3[A_1] + k_4[A_2])[B'] + k_3^*[A_1^*][B'] + k_4^*[A_2^*][B'] - R_3[E]\{(k_1[A_1] + k_2[A_2]) + k_1^*[A_1^*] + k_2^*[A_2^*]\} \quad (33)$$

$$\frac{d[F]}{dt} = (k_5[A_1] + k_6[A_2])[D] + k_5^*[A_1^*][D] + k_6^*[A_2^*][D] - [F]\{(k_7[A_1] + k_8[A_2]) + k_7^*[A_1^*] + k_8^*[A_2^*]\} \quad (34)$$

$$\frac{d[M]}{dt} = R_3[E]\{(k_1[A_1] + k_2[A_2]) + k_1^*[A_1^*] + k_2^*[A_2^*]\} \quad (35)$$

$$\frac{d[G]}{dt} = [F]\{(k_7[A_1] + k_8[A_2]) + k_7^*[A_1^*] + k_8^*[A_2^*]\} \quad (36)$$

The concentrations of the different species can be expressed in terms of conversion or fractional formation. Equations 37−50 define these variables. Aloph indicates allophanate (also repesented by M in the equations above).

$$p_A = 1 - \frac{[A]}{2[A]_0} \quad (37)$$

$$p_{A_1} = 1 - \frac{[A_1]}{2[A]_0} \quad (38)$$

$$p_{A_2} = 1 - \frac{[A_2]}{2[A]_0} \quad (39)$$

$$p_{A_1}* = 1 - \frac{[A_1^*]}{2[A]_0} \quad (40)$$

$$p_{A_2}* = 1 - \frac{[A_2^*]}{2[A]_0} \quad (41)$$

$$p_{B_T} = 1 - \frac{[B] + [B_f] + [B']}{f[B_f]_0 + 2[B']_0 + 2[B_2]_0} \quad (42)$$

$$p_{B_2} = 1 - \frac{[B]}{2[B_2]_0} \quad (43)$$

$$p_{B_2'} = 1 - \frac{[B']}{2[B_2']_0} \quad (44)$$

$$p_D = 1 - \frac{[D]}{2[D]_0} \quad (45)$$

$$p_E = \frac{[E]}{[B]_0} \quad (46)$$

$$p_F = \frac{[F]}{2[D]_0} \quad (47)$$

$$p_{Aloph} = \frac{[Aloph]}{2[D]_0} \quad (48)$$

$$p_G = \frac{[G]}{2[D]_0} \quad (49)$$

$$p_{U_T} = p_E + p_F + p_{Aloph} + p_G \quad (50)$$

Macosko−Miller Probabilistic Recursive Model. Although the methodology of the Macosko−Miller ap-

proach to the modeling of molecular weight averages and branching is well-established and several papers and textbooks describe the fundamentals of the method,[3,5,10−13,20−24] the key points of the method are outlined below.

The method uses the statistical law of conditional expectation, eq 51, to calculate the expected mass of a population of polymer molecules. To calculate the molar mass of an individual molecule, a monomer molecule unit attached to that polymer molecule is selected randomly. That monomer unit can be any of the isocyanate, diol, or "urethane" (reactive proton attached to the urethane group) monomers. The mass of the molecule is calculated by adding the mass of the molecule attached to one side of the reference unit to the mass attached to the other side of the unit. If the portion of the chain attached to that unit does not contain the reference unit as one moves along that side of the chain, then one is "looking out" from that reference unit. On the other hand, if the unit is included in the portion of the chain as one moves along that portion of the chain, then one is "looking in". When this procedure is applied to all of the chains present in the population and the expected (average) value of the mass is calculated, the result is the weight-average molecular weight of the population of polymer molecules.

$$E(Y) = E(Y|A)\,P(A) + E(Y|\bar{A})\,P(\bar{A}) \tag{51}$$

The idea is to calculate M_w directly by using eq 52, where the expected values of molar mass of the molecules are calculated using eq 51 and physical arguments regarding the probabilities of reaction, $P(A)$, or no reaction, $P(\bar{A})$. M_n can be calculated from its definition, given by eq 43, where m_t is total mass and N is the number of moles of molecules. Subscripts 0 and b account for initial and present conditions, respectively. M_X and w_X are molecular weight and mass fraction, respectively, of species X.

$$M_w = \sum_{i=1}^{N} w_{X_i} E(X_i) \tag{52}$$

where

$$w_{X_i} = \frac{M_{X_i} X_i}{\sum M_{X_i} X_i}$$

for $X_i = A_1, A_2, A_1^*, A_2^*, B, B', B_f, D, E, F, M, G$

$$M_n = \frac{m_t}{N_0 - N_b} \tag{53}$$

The core of the method is to calculate the expected mass values for each species. Using conditional probabilistic arguments and the concepts of looking in and looking out, eqs 54−69 are obtained. Gupta and Kumar[3] also used this methodology, but their nomenclature and explanations were not complete and clear enough in their text. Therefore, we started from the Macosko and Miller original publications.[10−12]

$$E(M_{A_1}) = E(M^{in}_{A_1}) + E(M^{out}_{A_1}) \tag{54}$$

$$E(M_{A_2}) = E(M^{in}_{A_2}) + E(M^{out}_{A_2}) \tag{55}$$

$$E(M_{A_1^*}) = E(M^{in}_{A_1^*}) + E(M^{out}_{A_1^*}) \tag{56}$$

$$E(M_{A_2^*}) = E(M^{in}_{A_1^*}) + E(M^{out}_{A_1^*}) \tag{57}$$

$$E(M_B) = E(M^{in}_B) + E(M^{out}_B) \tag{58}$$

$$E(M_{B'}) = E(M^{in}_{B'}) + E(M^{out}_{B'}) \tag{59}$$

$$E(M_{B_f}) = E(M^{in}_{B_f}) + (f_{B_f} - 1)E(M^{out}_{B_f}) \tag{60}$$

$$E(M_D) = E(M^{in}_D) + E(M^{out}_D) \tag{61}$$

$$E(M_E) = E(M^{in}_E) + (f_E - 1)E(M^{out}_E) \tag{62}$$

$$E(M_M) = E(M^{in}_M) + (f_M - 1)E(M^{out}_M) \tag{63}$$

$$E(M_F) = E(M^{in}_F) + (f_F - 1)E(M^{out}_F) \tag{64}$$

$$E(M_G) = E(M^{in}_G) + (f_G - 1)E(M^{out}_G) \tag{65}$$

$$E(M^{in}_{A_i}) = M_A + E(M^{out}_{A_i}), \quad A_i = A_1, A_2, A_1^*, A_2^* \tag{66}$$

$$E(M^{in}_{X_j}) = M_{X_j} + E(M^{out}_{X_j}), \quad X_j = B, B', B_f, D, E, F, M, G \tag{67}$$

$$E(M^{out}_{A_i}) = p_{A_i}\sum_j b_{X_j} E(M^{in}_{X_j}), \quad \text{where} \quad b_{X_i} = \frac{f_i X_i}{\sum_j f_j X_j} \tag{68}$$

$$E(M^{out}_{X_i}) = p_{X_i}\sum_j a_{A_j} E(M^{in}_{A_j}), \quad \text{where} \quad a_{A_i} = \frac{[A_i]}{\sum_j [A_j]} \tag{69}$$

Equations 54−69 for the expected masses of the different species looking in and looking out are interdependent. To produce explicit expressions for each variable, this system of simultaneous linear equations should be solved symbolically. To do so, the symbolic module of the mathematical package Matlab was used. After rearrangement of the expressions produced by Matlab, eqs 70−81 were obtained for expected values looking in and eqs 89−100 for expected values looking out. Although the main variables and symbols are explained within the text, the Nomenclature section provides a detailed description of their meaning.

$$E(M^{in}_{A_1}) = \frac{M_A(\phi_1\beta - 1) - p_{A_1}\gamma}{\alpha\beta - 1} \tag{70}$$

$$E(M^{in}_{A_2}) = \frac{M_A(\phi_2\beta - 1) - p_{A_2}\gamma}{\alpha\beta - 1} \tag{71}$$

$$E(M^{in}_{A_1^*}) = \frac{M_A(\phi_3\beta - 1) - p_{A_1^*}\gamma}{\alpha\beta - 1} \tag{72}$$

$$E(M^{in}_{A_1^*}) = \frac{M_A(\phi_3\beta - 1) - p_{A_1^*}\gamma}{\alpha\beta - 1} \tag{73}$$

$$E(M^{in}_B) = \frac{\alpha[M_B(\beta - p_B b_B) - p_B(\gamma - b_B M_B)] - (p_B M_A + M_B)}{\alpha\beta - 1} \tag{74}$$

$$E(M_{B'}^{in}) = \frac{\alpha[M_{B'}(\beta - p_{B'}b_{B'}) - p_{B'}(\gamma - b_{B'}M_{B'})] - (p_{B'}M_A + M_{B'})}{\alpha\beta - 1} \quad (75)$$

$$E(M_{B_f}^{in}) = \frac{1}{\alpha\beta - 1}\{\alpha[M_{B_f}(\beta - (f_{B_f} - 1)p_{B_f}b_{B_f}) - (f_{B_f} - 1)p_{B_f}(\gamma - (f - (f_{B_f} - 1)b_{B_f}M_{B_f})] - ((f_{B_f} - 1)p_{B_f}M_A + M_{B_f})]\} \quad (76)$$

$$E(M_D^{in}) = \frac{1}{\alpha\beta - 1}\{\alpha[M_D(\beta - p_D b_D) - p_D(\gamma - b_D M_D)] - (p_D M_A + M_D)\} \quad (77)$$

$$E(M_E^{in}) = \frac{1}{\alpha\beta - 1}\{\alpha[M_E(\beta - (f_E - 1)p_E b_E) - (f_E - 1)p_E(\gamma - b_E M_E)] - ((f_E - 1)p_E M_A + M_E)\} \quad (78)$$

$$E(M_F^{in}) = \frac{1}{\alpha\beta - 1}\{\alpha[M_F(\beta - (f_F - 1)p_F b_F) - (f_F - 1)p_F(\gamma - b_F M_F)] - ((f_F - 1)p_F M_A + M_F)\} \quad (79)$$

$$E(M_M^{in}) = \frac{1}{\alpha\beta - 1}\{\alpha[M_M(\beta - (f_M - 1)p_M b_M) - (f_M - 1)p_M(\gamma - b_M M_M)] - ((f_M - 1)p_M M_A + M_M)\} \quad (80)$$

$$E(M_G^{in}) = \frac{1}{\alpha\beta - 1}\{\alpha[M_G(\beta - (f_G - 1)p_G b_G) - (f_G - 1)p_G(\gamma - b_G M_G)] - ((f_G - 1)p_G M_A + M_G)\} \quad (81)$$

In the above equations, α, β, γ, and ϕ_1−ϕ_4 are defined in terms of the conversions and molar fractions of the different species, as shown in eqs 82−88.

$$\alpha = p_{A_1}a_{A_1} + p_{A_1^*}a_{A_1^*} + p_{A_2}a_{A_2} + p_{A_2^*}a_{A_2^*} \quad (82)$$

$$\beta = p_B b_B + p_{B'}b_{B'} + (f_{B_f} - 1)p_{B_f}b_{B_f} + p_D b_D + (f_E - 1)p_E b_E + (f_F - 1)p_F b_F + (f_M - 1)p_M b_M + (f_G - 1)p_G b_G \quad (83)$$

$$\gamma = b_B M_B + b_{B'}M_{B'} + b_{B_f}M_{B_f} + b_D M_D + b_E M_E + b_F M_F + b_M M_M + b_G M_G \quad (84)$$

$$\phi_1 = p_{A_1^*}a_{A_1^*} + p_{A_2}a_{A_2} + p_{A_2^*}a_{A_2^*} - p_{A_1}(1 - a_{A_1}) \quad (85)$$

$$\phi_2 = (p_{A_1} - p_{A_2})a_{A_1} + (p_{A_1^*} - p_{A_2})a_{A_1^*} + (p_{A_2^*} - p_{A_2})a_{A_2^*} \quad (86)$$

$$\phi_3 = (p_{A_1} - p_{A_1^*})a_{A_1} + (p_{A_2} - p_{A_1^*})a_{A_2} + (p_{A_2^*} - p_{A_1^*})a_{A_2^*} \quad (87)$$

$$\phi_4 = (p_{A_1} - p_{A_2^*})a_{A_1} + (p_{A_2} - p_{A_2^*})a_{A_2} + (p_{A_1^*} - p_{A_2^*})a_{A_1^*} \quad (88)$$

$$E(M_{A_1}^{out}) = \frac{p_{A_1}(\beta M_A + \gamma)}{1 - \alpha\beta} \quad (89)$$

$$E(M_{A_2}^{out}) = \frac{p_{A_2}(\beta M_A + \gamma)}{1 - \alpha\beta} \quad (90)$$

$$E(M_{A_1^*}^{out}) = \frac{p_{A_1^*}(\beta M_A + \gamma)}{1 - \alpha\beta} \quad (91)$$

$$E(M_{A_2^*}^{out}) = \frac{p_{A_2^*}(\beta M_A + \gamma)}{1 - \alpha\beta} \quad (92)$$

$$E(M_B^{out}) = \frac{p_B(M_A + \alpha\gamma)}{1 - \alpha\beta} \quad (93)$$

$$E(M_{B'}^{out}) = \frac{p_{B'}(M_A + \alpha\gamma)}{1 - \alpha\beta} \quad (94)$$

$$E(M_{B_f}^{out}) = \frac{p_{B_f}(M_A + \alpha\gamma)}{1 - \alpha\beta} \quad (95)$$

$$E(M_D^{out}) = \frac{p_D(M_A + \alpha\gamma)}{1 - \alpha\beta} \quad (96)$$

$$E(M_E^{out}) = \frac{p_E(M_A + \alpha\gamma)}{1 - \alpha\beta} \quad (97)$$

$$E(M_F^{out}) = \frac{p_F(M_A + \alpha\gamma)}{1 - \alpha\beta} \quad (98)$$

$$E(M_M^{out}) = \frac{p_M(M_A + \alpha\gamma)}{1 - \alpha\beta} \quad (99)$$

$$E(M_G^{out}) = \frac{p_G(M_A + \alpha\gamma)}{1 - \alpha\beta} \quad (100)$$

Given the fact that experimental data for reaction viscosity were available, a correlation between viscosity and weight-average molecular weight, eq 101, was used.

$$\eta = k' M_w^{\,n}[U]^m \quad (101)$$

Results and Discussion

Parameter Estimation Procedure. The polymerization system studied in this paper is the copolymerization of MDI/polyester/1,4-butanediol. Initial values for the kinetic and model parameters were taken from the literature or guessed (values of the same order of magnitude as the reported values for other constants). The ranges of variation of the parameters were established from parameter-sensitivity analyses carried out with the simulation program.

Final values for the unknown or uncertain model parameters were estimated using the method of "error in variables", a weighted multivariable nonlinear regression procedure, using experimental data from Castro et al.[21] The simulations and parameter estimation calculations were carried out with a Fortran 90 implementation of the model equations. All of the unknown parameters were estimated simultaneously using all of the experimental data available (hydroxyl conversion, weight-average molecular weight, and viscosity).

The polymerization conditions, molecular weights of the different reactive species, and estimated kinetic constants are summarized in Tables 1−3.

Description of the Experimental Techniques.[30] The experimental data used to validate the model proposed in this paper were obtained by Castro.[30] Some details of his experimental procedures and characterization techniques are included here to provide a better idea of the reliability of the experimental data.

Table 1. Initial Conditions for Copolymerization of MDI, Polyester, and 1,4-Butanediol

parameter	value	units
temperature	30, 50, or 90	°C
$[A_1A_2]_0$	1.5261	mol L^{-1}
$[B_2]_0$	0.3052	mol L^{-1}
$[B'_2]_0$	1.221	mol L^{-1}

Table 2. Molecular Weight Constants

parameter	value	units or comments
M_A	250	g mol^{-1}
M_B	2500	g mol^{-1}
$M_{B'}$	90	g mol^{-1}
M_E	59	g mol^{-1}
M_F	58	g mol^{-1}
M_M (M_{Aloph})	101	g mol^{-1}
f_E	3	see Figure 1 and text
f_M	4	see structure of allophanate unit in Figure 3 and text
k'	2.93×10^{-13}, 1.52×10^{-15}, 5.17×10^{-15}	Pa s (at 30, 50, and 90 °C, respectively), using EVM (zero included in confidence intervals)
N	2.21	estimated using EVM (zero included in confidence intervals)
M	13	estimated using EVM (zero included in confidence intervals)

The isocyanate stream of a small laboratory reaction injection molding (RIM) machine contained 100 wt % of a liquid form of 4,4′-diphenyl methane diisocyanate. The polyol stream contained 1,4-butanediol (BDO) and a long polyol which was a polypropylene oxide capped with ethylene oxide. The weight percentages of polyol and BDO in the polyol stream were 85 and 15, respectively. A stoichiometric ratio of 1.0 was used.

The kinetics of the polyurethane formation reaction was determined using the temperature rise during adiabatic heating or the "quasi-adiabatic reactions" method. To use this method, the following assumptions are necessary: (i) the system is homogeneous and well-mixed, (ii) no diffusion-controlled effects arise as the molecular weight increases, (iii) the heat of reaction is constant, and (iv) the system follows simple second-order kinetics and Arrhenius temperature dependence of the rate constant. A small laboratory RIM machine was used. For the reaction, 50−70 g of reaction mixture was injected into a double styrene coffee cup. A small copper thermocouple was inserted through the walls of the cup. Another similar thermocouple was placed near the machine outlet to measure the initial temperature. The fill cycle took 5 s, after which the cup was covered with a large cork stopper. The temperature was recorded using real-time data acquisition.

Isothermal viscosity measurements were made with a Rheometrics mechanical spectrometer using a 50-mm-diameter cone and plate with a cone angle of 0.04 rad. The materials were preheated in a water bath. The polyols were preweighed, and the isocyanate was added by volume. The components were mixed for 30 s in a mechanical mixer, and then a 1.5-mL sample was transferred to the cone and plate, from which the viscosity rise as a function of time was obtained.

The weight-average molecular weight data reported by Castro[30] were obtained using an equation developed by López-Serrano et al.[20] That equation is indeed based on the Macosko−Miller approach, considering three monomers as in this paper, but neglecting branching and cross-linking. Experimental values of the extent of reaction were inserted into that equation to obtain the corresponding M_w values.

Comparison of Simulated versus Experimental Data. Figure 4 shows predicted best-fit profiles and experimental data for 1,4-butanediol (BDO) hydroxyl conversion at 30, 50, and 90 °C. The agreement is fairly good up to about 70% BDO hydroxyl conversion. After that, the model calculations are higher than the experimental data. Predictions of number- and weight-average molecular weights are compared with the values reported by Castro[30] at the same three temperatures in Figure 5. It is strange to observe that the model predictions in the three cases show a maximum in M_w and the absence of gelation. Castro[30] reported that gelation occurred at approximately 85% hydroxyl conversion, but he based his statement on the observation of a plot of viscosity versus conversion that seemed to diverge at around that conversion level. However, no specific experiments for gel content quantification or direct molecular weight measurements were reported in Castro's work.[30] The calculated maximum in M_w observed in Figure 5 coincided with the depletion of hydroxyl functional groups from the chain extender (BDO).

Without knowing for sure whether gelation takes place, it is difficult to draw additional conclusions from Figure 5. The agreement between the model predictions and the data reported by Castro[30] is good at 30 and 90 °C. The predicted profile at 50 °C deviates from the reported data in the intermediate BDO hydroxyl conversion range. One point worth mentioning here is that the values of M_w reported by Castro[30] are not direct measurements using a valid technique for nonlinear polymer molecules, but calculations using experimental data of BDO hydroxyl conversion and a model that is not valid for nonlinear polymer molecules. As mentioned in the Description of Experimental Techniques section of this paper, the values of M_w reported by Castro[30] were calculated with the linear version of the Macosko−Miller model.[20] In this paper, a nonlinear version of that model was used to calculate molecular weight development and prediction of the gelation point.

Figure 6 shows model-predicted and experimental viscosity data for the three temperatures considered in this section. The agreement seems to be quite good, but considering that the correlation for viscosity contains three parameters, as shown in eq 101, and the fact that estimation of those parameters provides unreliable estimates (confidence intervals including zero), it is concluded that the same good agreement could have been obtained with different combinations of the viscosity parameters. In other words, the model could be adequate, but the experimental data available are not sufficient to give reliable estimates of the parameters. The peaks observed in the predicted profiles are related to the maximum peaks in the M_w versus time profiles observed in Figure 5.

Although it is not possible to determine with certainty whether gelation occurred in the experimental system of Castro,[30] the exponential-like increase on viscosity seems to indicate that gelation could have occurred at some point. As mentioned before, the model predictions shown in Figures 5 and 6 indicate that gelation does not occur in this system for the polymerization conditions used by Castro.[30] The profiles shown in Figures 5 and 6 were calculated assuming that the urethane functional group behaves as a monomer of functionality 3 (see Figure 1) and that the allophanate functional group behaves as a monomer of functionality 4, because

Table 3. Kinetic Rate Constants

parameter	value at 30 °C	value at 50 °C	value at 90 °C	units or comments
k_1	0.029 24	0.0795	0.45	L mol^{-1} min^{-1}, Hager et al.[29]
k_2	0.029 24	0.0795	0.45	L mol^{-1} min^{-1}, assumed equal to k_1
k_3	0.0106 ± 0.0002	0.0168 ± 0.0003	0.3163 ± 0.02	L mol^{-1} min^{-1}, EVM
k_4	0.0106 ± 0.0002	0.0168 ± 0.0003	0.3163 ± 0.02	L mol^{-1} min^{-1}, assumed equal to k_3
k_1^*	0.0001	0.0068 ± 0.0003	1.25×10^{-2}	L mol^{-1} min^{-1}, EVM (zero included in confidence interval at 30 and 90 °C)
k_2^*	0.0001	0.0068 ± 0.0003	1.25×10^{-2}	L mol^{-1} min^{-1}, assumed equal to k_1^*
k_3^*	0.0072	0.0263 ± 0.0008	0.019	L mol^{-1} min^{-1}, (zero included in confidence interval at 30 and 90 °C)
k_4^*	0.0072	0.0263 ± 0.0008	0.019	L mol^{-1} min^{-1}, assumed equal to k_3^*
R_3	0.002 63	0.002 63	0.002 63	Gupta and Kumar[3]

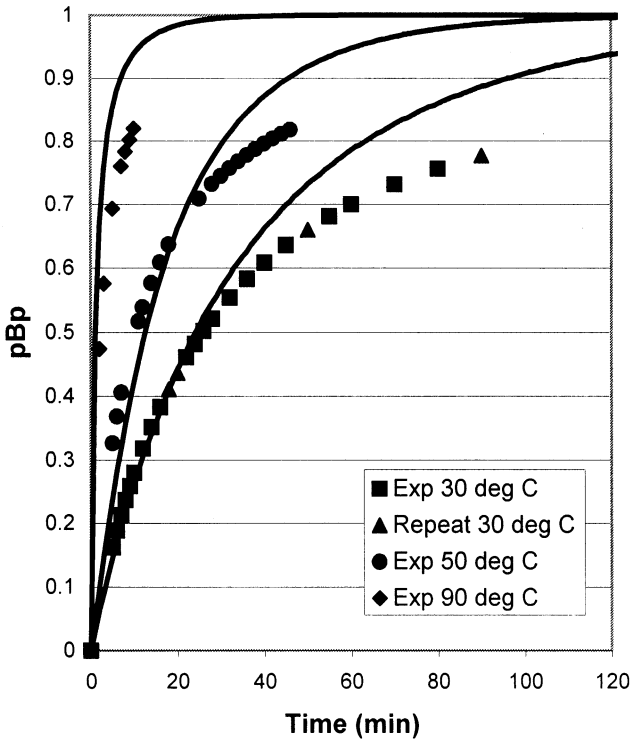

Figure 4. Copolymerization of MDI/polyol/1,4-butanediol. Comparison of model predictions and experimental data on polyol hydroxyl conversion at 30, 50, and 90 °C for initial conditions of Table 1.

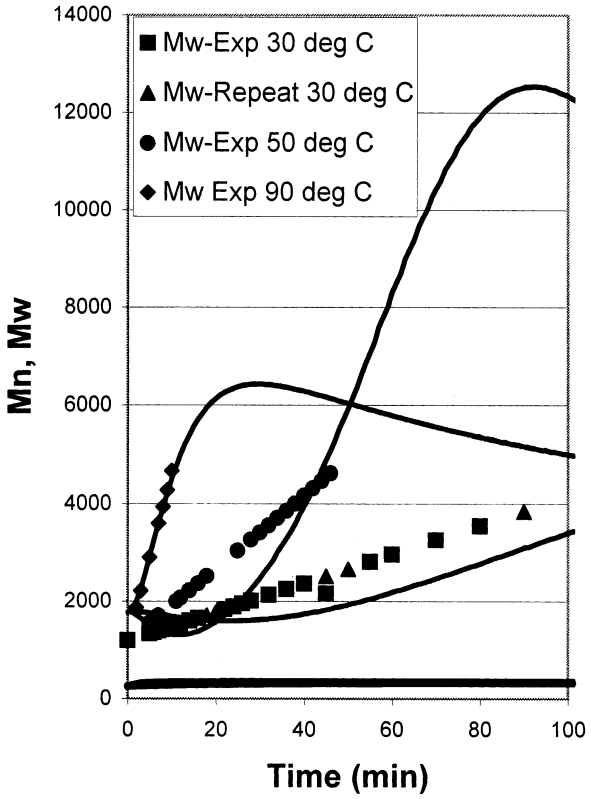

Figure 5. Copolymerization of MDI/polyol/1,4-butanediol. Comparison of model predictions of number- and weight-average molecular weights and calculated data of Castro[30] for weight-average molecular weight versus time at 30 (squares), 50 (circles), and 90 °C (diamonds) for initial conditions of Table 1.

the allophanate unit has two substituted segments from the original polyurethane chain, an additional segment obtained from the attack of the isocyanate group from another chain to the proton of the urethane group of the reference polyurethane chain, and another proton that can be attacked by another isocyanate functional group, as indicated in the reaction mechanism shown in Figure 3. All together, the different segments that can be attached to an allophanate unit number four, which is the assumed functionality.

It has been proposed that polyurethane networks having trifunctional units can lead to thermal and mechanical properties that can only be explained if the polymer network contains cross-linking units of functionality greater than 3. These higher-order multifunctional units are explained as an association of other units that form "hard clusters". These clusters can then behave as units of functionality 4 or higher.[31] Figure 7 shows a cluster of functionality 4, obtained by the association of two units of functionality 3. If it is considered that the reacting system studied in this paper can lead to nonlinear polymer molecules with urethane units of functionality 3 (Figure 1) and hard clusters of functionality 4 (Figure 7), then the average functionality to be used in our model should be higher than 3. Figure 8 shows simulations of the weight-average molecular weight with the model proposed here, using different average functionalities of the urethane units, in the range of 3−4. The system presented in Figure 8 is the one at 50 °C, which presented the higher deviations shown in Figures 5 and 6. The solid line in Figure 8 is the reference case obtained with $f_E = 3$. The long dashed (—) line is the case with $f_E = 4$, that is, with all of the urethane units assumed to form hard clusters of functionality 4. Gelation in this case is predicted to occur at approximately 22 min of reaction time. The profiles between these two limits show that gelation is possible. The gelation point depends on the value of the average functionality. According to the calculations shown in Figure 8, the lowest value of f_E that can lead to gelation is 3.11. Values lower than that will produce

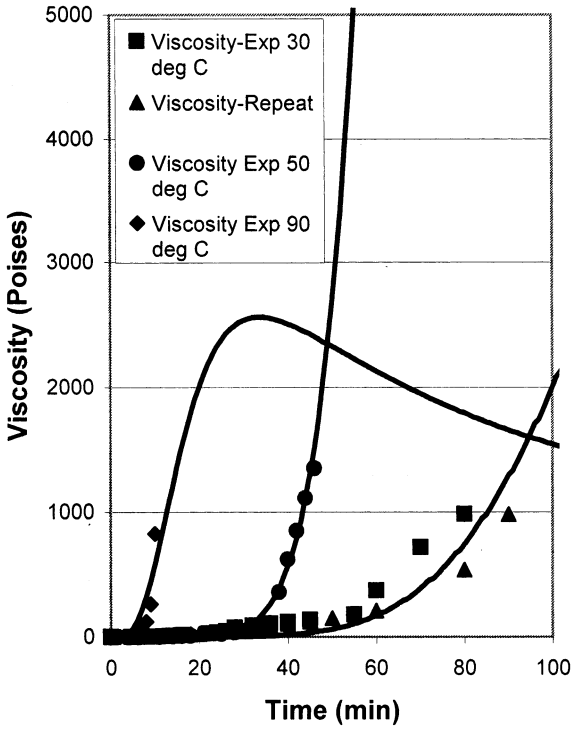

Figure 6. Copolymerization of MDI/polyester/1,4-butanediol. Comparison of model predictions and experimental data of reactive mixture viscosity at 30, 50, and 90 °C for initial conditions of Table 1.

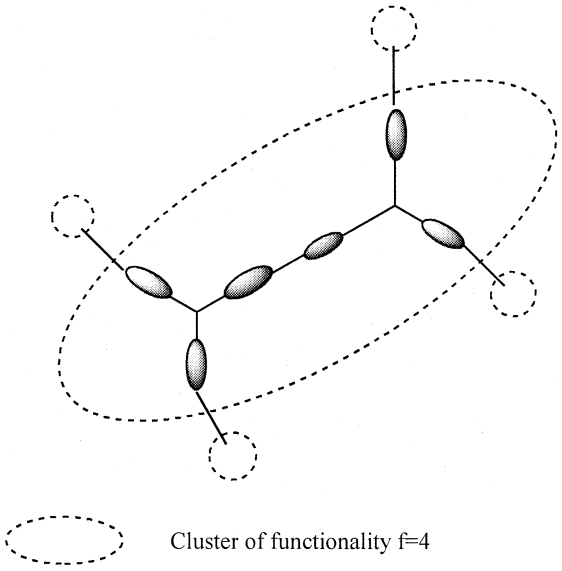

Figure 7. Schematic representation of a hard cluster of functionality 4.

profiles with higher weight-average molecular weights than those obtained with $f_E = 3$, but without forming a polymer network. The intermediate profiles with f_E between 3 and 3.11 were calculated but are not shown in Figure 8.

Effect of the Stoichiometric Imbalance Ratio on Molecular Weight Development. Figures 9 and 10 show the predicted effect of the stoichiometric imbalance ratio (SIR) on the weight-average molecular weight and the BDO hydroxyl conversion, respectively, at 50 °C. The reference case shown with the solid line in Figure 9 was calculated using SIR = 1 and $f_E = 3$ (no hard clusters considered). First, it was assumed that the

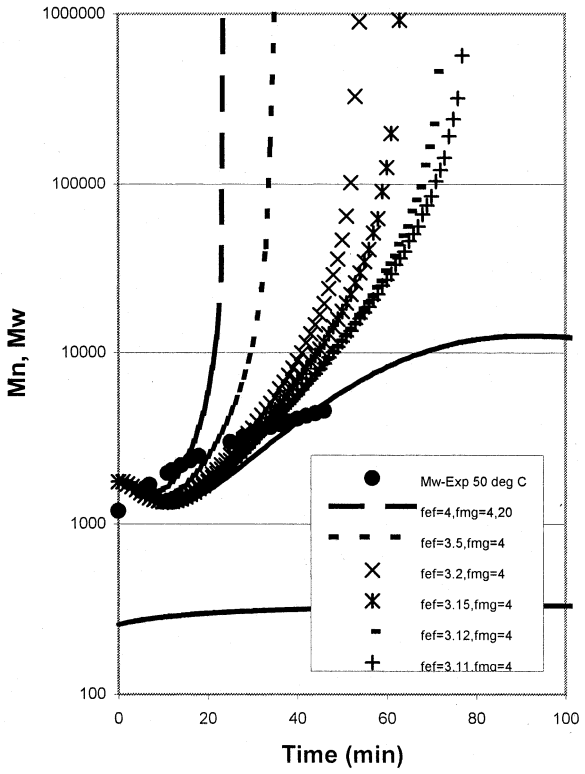

Figure 8. Effect of hard-cluster content (represented by increased equivalent functionality of the urethane unit) on molecular weight development and occurrence of the gelation point.

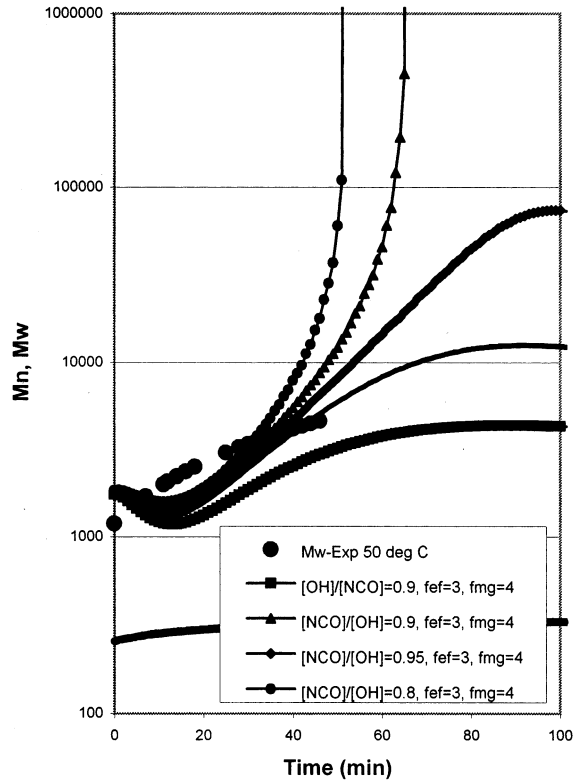

Figure 9. Effect of the stoichiometric imbalance ratio (SIR) on molecular weight development in the copolymerization of MDI/polyol/1,4-butanediol at 50 °C. Values of SIR and functionalities shown in plot legend.

isocyanate functional groups were in excess, with a SIR = 0.9. In this case, the model predicts a reduction in the weight-average molecular weight compared to the

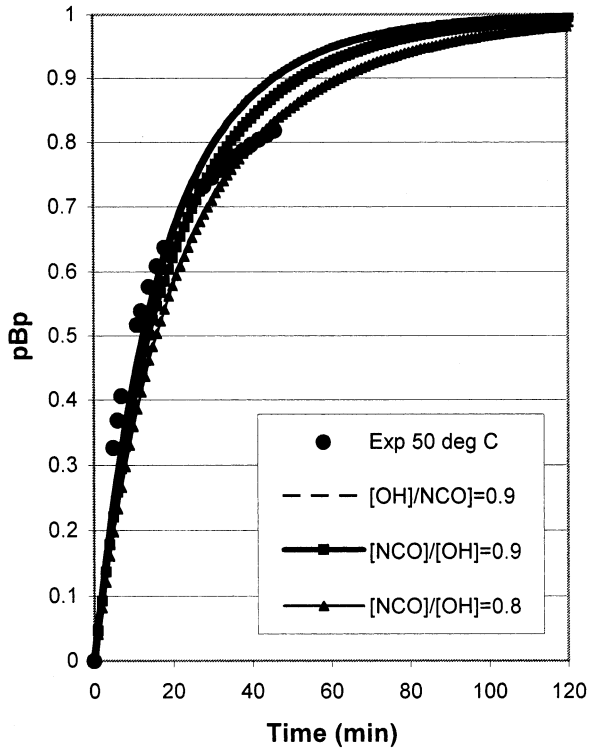

Figure 10. Effect of the stoichiometric imbalance ratio (SIR) on polyol hydroxyl conversion in the copolymerization of MDI/polyol/1,4-butanediol at 50 °C. Definition and values of SIR are indicated in plot legend.

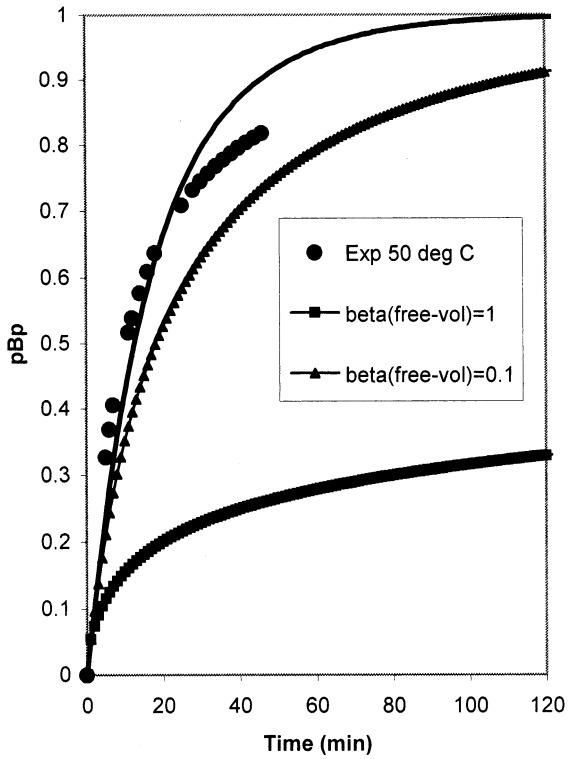

Figure 11. Effect of diffusion-controlled kinetics on polyol hydroxyl conversion in the copolymerization of MDI/polyol/1,4-butanediol at 50 °C. Beta(free-vol) in the plot legend refers to parameter β of eq 102.

stoichiometric case, without gelation taking place (profile with squares over a thin solid line). Then, it was assumed that the overall hydroxyl functional groups were in excess (SIR = [NCO]/[OH]), and simulations with different values of SIR were produced. It is observed from the model simulations that, when the hydroxyl functional groups are in excess, a reduction of the SIR increases the weight-average molecular weight profiles and gelation can take place. The lower the value of SIR, the sooner gelation occurs, at least in the SIR range of 0.8−1.0, when the hydroxyl functional groups are in excess.

Figure 10 shows that a reduction of the SIR when the isocyanate functional groups are in excess does not significantly affect the BDO hydroxyl conversion, because the two profiles overlap. However, when the overall hydroxyl functional groups are in excess, a reduction of the SIR causes a reduction of the conversion of hydroxyl functional groups from the chain extender (BDO).

These simulations show the importance of controlling the SIR in molecular weight development. What could be considered "minor" errors in mass measurement could have major consequences for reactor operation, particularly when gelation is not desired.

Inclusion of Diffusion-Controlled Effects in the Reaction Kinetics. Another possible explanation to the difference between the model predictions and the experimental/calculated data of Castro[30] is the fact that diffusion-controlled effects were not considered in the original model. Diffusion control of chemical reactions is a well-known phenomenon in polymer science. Whether a given chemical reaction is controlled by diffusion depends on the relative rate of the diffusion process (translational diffusion of species or segmental diffusion) and the intrinsic chemical reaction resulting in bond formation or scission.[32] Diffusion-controlled effects have been modeled using free-volume theory in both free-radical (e.g., ref 33) and step-growth polymerizations.[32,34−35]

In this paper a "serial approach" instead of a "parallel approach" was used to calculate diffusion-controlled kinetic rate constants. A detailed discussion of the series and parallel approaches for diffusion-controlled reactions is presented in Vivaldo-Lima et al.[33] All of the kinetic rate constants used in this paper (k_1, k_2, k_3, k_4, k_1^*, k_2^*, k_3^*, and k_4^*) were corrected for diffusion-controlled effects using eq 102, where V_f is fractional free-volume, calculated using eq 103. The remaining terms are defined in the nomenclature section of this paper.

$$k_i = k_i^0 \exp\left[-\beta_i\left(\frac{1}{V_f} - \frac{1}{V_f^0}\right)\right] \qquad (102)$$

$$V_f = \sum_i^N [0.025 + \alpha_i(T - T_{gi})]\frac{V_i}{V_t}, \quad i = A_1A_2, B_2, B', \text{polymer} \qquad (103)$$

Figures 11 and 12 show the effects of diffusion-controlled reactions on BDO hydroxyl conversion and molecular weight development, respectively. The results presented in these figures correspond to the polymerization at 50 °C. The free-volume parameters used to obtain these profiles are summarized in Table 4. When all of the reactions have the same free volume dependence (the same values of the overlap factor, β), the rate of polymerization is reduced, and the weight-average molecular weight attained is also reduced. The magnitude of these changes depends on the value of β used, as shown in Figures 11 and 12. These results make

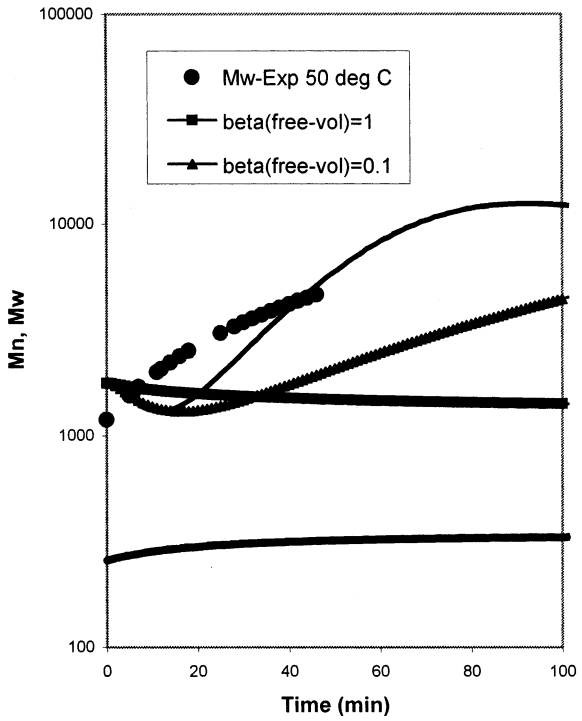

Figure 12. Effect of diffusion-controlled kinetics on polyurethane molecular weight development (M_n and M_w) in the copolymerization of MDI/polyol/1,4-butanediol at 50 °C. Beta(free-vol) in the plot legend refer to parameter β of eq 102.

Table 4. Free-Volume Parameters for Diffusion-Controlled Effects

parameter	values	comments
β, dimensionless	0.1 and 1[a]	assumed the same for all reactions
T_{gi},[b] °C	−100, 57, −100, 57	guessed, ref 36, guessed, ref 36
α_i,[b] °C^{-1}	0.001, 0.000 48, 0.001, 0.000 48	guessed, ref 34, guessed, ref 34

[a] See Figures 11 and 12. [b] i = A_1A_2, B_2, B_2', polymer.

sense, because a reduction in the mobility of the chains makes their growth more difficult. In free-radical polymerization, the observed effect is the opposite, because there is a competition between propagation (growth of chains) and termination (cessation of chain growth) and termination is more significantly affected by diffusion-controlled effects.

For the specific system studied here (nonlinear polyurethane production from polyol, 1,4-butanediol, and MDI at 50 °C), the inclusion of diffusion-controlled effects in the model equations did not improve the agreement with the calculated data for M_w in Castro.[30] On the contrary, lower conversions and weight-average molecular weights were obtained. However, Figures 11 and 12 show that, if diffusion-controlled effects are present, their effects on BDO hydroxyl conversion and weight-average molecular weight can be significant.

Concluding Remarks

A mathematical model of intermediate degree of complexity for kinetics and molecular weight development in polyurethane production, considering crosslinking and gelation due to allophanate formation, has been developed. The degree of complexity of the model could be reduced by making use of the recursive probabilistic methodology of Macosko and Miller.[10−12] An important aspect of the model is the removal of the assumption of equal reactivities of functional groups.

Although the experimental data used to validate the model could not be reproduced adequately, it was demonstrated that some model assumptions used by the authors who generated the experimental data and some theoretical considerations, such as the existence of hard clusters in polyurethane polymer networks, can satisfactorily explain those deviations.[31]

Diffusion-controlled effects on the reaction kinetics of polyurethane production were included in the model presented here. Although the simulations presented here seemed to indicate that diffusion-controlled effects were not present in our system, it was shown that they could have a pronounced effect on the predicted rate of polymerization and molecular weight development. The importance of those effects could not be assessed in detail given the limitations of the experimental data used in this paper (model dependence assumptions regarding the weight-average molecular weight data).

The predictive power of the model, as well as its low degree of complexity, make it attractive for industrial applications or for more complex processes, such as reactive processing, where the complicated flow equations make it necessary to have the simplest possible kinetic model.

This model can be considered as an intermediate approach between the simplistic kinetic models for step-growth polymerization available in the literature (e.g., refs 22−26) and the more sophisticated gelation theories.

Acknowledgment

The authors acknowledge financial support from the National Council for Science and Technology (CONACyT) of Mexico and UNAM through Projects 31170-U and PAPIIT IN120599, respectively, granted to Professor E. Vivaldo-Lima. The assistance of Mr. Gabriel Jaramillo-Soto, a graduate student at UNAM, in redoing some of the calculations for the revised manuscript is greatly appreciated.

Nomenclature

[ ], [ ]$_0$ = concentration, where subscript 0 indicates value at initial conditions, mol L^{-1}
A = isocyanate functional group
A_2 = diisocyanate molecule
a_{A_i} = molar fraction of isocyanate functional groups, as defined in eq 69
Aloph = allophanate functional group (also represented by M)
B = hydroxyl functional group
B_2 = diol molecule of high molecular weight (polyol)
B_2' = diol molecule of low molecular weight (1,4-butanediol)
B_f = multiol molecule with f hydroxyl functional groups
BDO = 1,4-butanediol
b_{X_i} = quantity defined in eq 68
D = amine functional group
D_2 = diamine molecule
E = urethane functional group
$E(X_i)$ = expected mass of species X_i, kg kmol^{-1}
F = urea functional group
f_{X_i} = functionality of species X_i, X_i = E, F, G, M
k' = proportionality constant to correlate zero-shear viscosity, molecular weight, and total polymer concentration, as shown in eq 101, Pa s

k_i, k_i^* = kinetic rate constants, where superscript * indicates reactivity of a functional group bound to a polymer molecule and subscript or superscript 0 denotes value at initial conditions, L mol^{-1} min^{-1}
m = adjustable parameter defined in eq 101
m_t = total mass, kg
M = allophanate functional group (also represented by Aloph)
M_n = number-average molecular weight, kg kmol^{-1}
M_X = molar mass of species X, kg kmol^{-1}
M_w = weight-average molecular weight, kg kmol^{-1}
n = adjustable parameter defined in eq 101
N_0, N_b= number of molecules at initial and present conditions, respectively
G = biuret functional group
p_X = extent of reaction (probability of reaction) of species X, as defined in eqs 37−50 of the text
R_3 = proportionality constant between rates of allophanate and urethane formation
t = time, min
T = temperature, °C
T_{gi} = glass transition temperature of component i, °C
[U_T] = total polymer concentration, mol L^{-1}
V_f = fractional free volume, dimensionless
V_i = volume of species i, L
V_t = total volume, L
w_X = mass fraction of species X, as defined in eq 52

Greek Letters

α = intermediate variable in the Macosko−Miller model defined by eq 82
α_{X_i} = thermal expansion coefficient of species X_i, X_i = A_2, B_2, B_2', polymer, °C^{-1}
β = intermediate variable in the Macosko−Miller model defined by eq 83
β_i = overlap factor for reaction i, used to account for the fact that the same free volume is available to several molecules and also for separation once the molecules are together
ϕ_i = intermediate variables in the Macosko−Miller model, i = 1, 2, 3, 4, as defined in eqs 85−88
γ = intermediate variable in the Macosko−Miller model defined by eq 84

Literature Cited

(1) Frisch, K. C. Historical Developments of Polyurethanes. In *60 Years of Polyurethanes*; Kresta, J. E., Eldred, E. W., Eds.; Technomic Publishing Co., Inc.: Detroit, MI, 1998; pp 1−21.

(2) Zdrahala, R. J. Polyurethanes in Biomedical Applications: Promises of the Past, Present Realities and Vibrant Future. In *60 Years of Polyurethanes*; Kresta, J. E., Eldred, E. W., Eds.; Technomic Publishing Co., Inc.: Detroit, MI, 1998; pp 304−323.

(3) Gupta, S. K.; Kumar, A. *Reaction Engineering of Step Growth Polymerization*; Plenum Press: New York, 1987.

(4) Hamielec, A. E.; Tobita, H. Polymerization Processes. In *Ullmann's Encyclopedia of Industrial Chemistry*; VCH Publishers, Inc.: New York, 1992; Vol. A21, pp 305−428.

(5) Dotson, N. A.; Galván, R.; Laurence, R. L.; Tirrell, M. *Polymerization Process Modeling*; VCH Publishers, Inc.: New York, 1996.

(6) Flory, P. J. Molecular Size Distribution in Three-Dimensional Polymers. I. Gelation. *J. Am. Chem. Soc.* **1941**, *63*, 3083−3090.

(7) Flory, P. J. Molecular Size Distribution in Three-Dimensional Polymers. II. Trifunctional Branching Units. *J. Am. Chem. Soc.* **1941**, *63*, 3091−3100.

(8) Stockmayer, W. H. Theory of Molecular Size Distribution and Gel Formation in Branched-Chain Polymers. *J. Chem. Phys.* **1943**, *11* (2), 45−55.

(9) Stockmayer, W. H. Theory of Molecular Size Distribution and Gel Formation in Branched Polymers II. General Cross Linking. *J. Chem. Phys.* **1944**, *12* (4), 125−131.

(10) Macosko, C. W.; Miller, D. R. A New Derivation of Average Molecular Weights of Nonlinear Polymers. *Macromolecules* **1976**, *9* (2), 199−206.

(11) Miller, D. R.; Macosko, C. W. A New Derivation of Post Gel Properties of Network Polymers. *Macromolecules* **1976**, *9* (2), 206−211.

(12) Miller, D. R.; Macosko, C. W. Average Property Relations for Nonlinear Polymerization with Unequal Reactivity. *Macromolecules* **1978**, *11* (4), 656−662.

(13) Shiau, L.-D. An Extended Study on the Average Molecular Weights of Nonlinear Polymers. *Macromolecules* **1995**, *28*, 6273−6277.

(14) Gordon, M. Good's Theory of Cascade Processes Applied to the Statistics of Polymer Distributions. *Proc. R. Soc. A* **1962**, *268*, 240−259.

(15) Sekkar, V.; Rama Rao, M.; Krishnamurthy, V. N.; Jain, S. R. Modeling of Polyurethane Networks Based on Hydroxy-Terminated Polybutadiene and Poly(12-hydroxy stearic acid-*co*-TMP) Ester Polyol: Correlation of Network Parameters with Mechanical Properties. *J. Appl. Polym. Sci.* **1996**, *62*, 2317−2327.

(16) Dušek, K.; Špirková, M.; Havlíček, I. Network Formation of Polyurethanes Due to Side Reactions. *Macromolecules* **1990**, *23* (6), 1774−1781.

(17) Budinski-Simendiè, J.; Petroviè, Z. S.; Ilavsky, M.; Dušek, K. Effect of the Ratio of Reactive Groups on Gelation and Cyclization During Polyurethane Network Formation. *Polymer* **1993**, *34* (24), 5157−5162.

(18) Dušek, K.; Pascault, J.-P.; Špirková, M.; Somvársky, J. Polyurethane Networks and Chemical Clusters. In *60 Years of Polyurethanes*; Kresta, J. E., Eldred, E. W., Eds.; Technomic Publishing Co., Inc.: Detroit, MI, 1998; pp 143−160.

(19) Petrovič, Z. S.; MacKnight, W. J. The application of size exclusion chromatography equipped with RI and LALLS detectors to study network formation. *Polym. Bull.* **1991**, *27*, 281−287.

(20) López-Serrano, F.; Castro, J. M.; Macosko, C. W.; Tirrell, M. Recursive Approach to Copolymerization Statistics. *Polymer* **1980**, *21*, 263−273.

(21) Castro, J. M.; López-Serrano, F.; Camargo, R. E.; Macosko, C. W.; Tirrell, M. Onset of Phase Separation in Segmented Urethane Polymerization. *J. Appl. Polym. Sci.* **1981**, *26*, 2067−2076.

(22) Miller, D. R.; Sarmoria, C. "In−Out" Recursive Probability Modeling of Branched Step-Growth Polymerizations. *Polym. Eng. Sci.* **1998**, *38* (4), 535−557.

(23) Sarmoria, C.; Miller, D. R. Spanning-tree models for A_f homopolymerizations with intramolecular reactions. *Comput. Theor. Polym. Sci.* **2001**, *11*, 113−127.

(24) Castro, J. M.; Macosko, C. W.; Perry, S. J. Viscosity Changes During Urethane Polymerization with Phase Separation. *Polym. Commun.* **1984**, *25*, 82−87.

(25) Hyun, M. E.; Kim, S. C. A Study on the Reactive Extrusion Process of Polyurethane. *Polym. Eng. Sci.* **1988**, *28* (11), 743−757.

(26) Park, K. C.; Kim, S. C. Bulk Polymerization of Polyurethane under High Pressure. *J. Appl. Polym. Sci.* **1990**, *39*, 639−647.

(27) Ando, T. Effect of Reaction Temperature on Polyurethane Formation in Bulk. *Polymer J.* **1993**, *25* (11), 1207−1209.

(28) Król, P. Generalization of Kinetics in the Reaction of Isocyanates and Polyols for Modeling a Process-Yielding Linear Polyurethane, 1. *J. Appl. Polym. Sci.* **1995**, *57*, 739−749.

(29) Hager, S. L.; MacRury, T. B.; Gerkin, R. M.; Critchfield, F. E. *ACS Polym. Prepr.* **1980**, *21* (2), 298.

(30) Castro, J. M. Ph.D. Thesis, Department of Chemical Engineering, University of Minnesota, Minneapolis, MN, 1981.

(31) Nabeth, B; Pascault, J. P.; Dusek, K. Concept of hard clusters in the interpretation of thermal and mechanical properties of polyurethane and polyurethane acrylate networks. *J. Polym. Sci. B: Polym. Phys.* **1996**, *34* (6), 1031−1054.

(32) Dusek, K.; Havlicek, I. Diffusion controlled kinetics of cross-linking. *Prog. Org. Coat.* **1993**, *22*, 145−159.

(33) Vivaldo-Lima, E.; Hamielec, A. E.; Wood, P. E. Auto-acceleration effect in free radical polymerization. A comparison of the CCS and MH models. *Polym. React. Eng.* **1994**, *2* (1&2), 17−85.

(34) Sanford, W. M.; McCullough, R. L. A free-volume-based approach to modeling thermoset cure behavior. *J. Polym. Sci. B: Polym. Phys.* **1990**, *28*, 973−1000.

(35) Simon, S. L.; Gillham, J. K. Reaction kinetics and TTT cure diagrams for off-stoichiometric ratios of a high-T_g epoxy/amine system. *J. Appl. Polym. Sci.* **1992**, *46*, 1245−1270.

(36) Andrews, R. J.; Grulke, E. A. Glass Transition Temperatures of Polymers. In *Polymer Handbook*, 4th ed.; Brandrup, J., Immergut, E. H., Grulke, E. A., Eds.; John Wiley & Sons, Inc.: New York, 1999; Section VI, pp 253−254.

Received for review September 5, 2001
Revised manuscript received July 24, 2002
Accepted July 29, 2002

IE010742G